Hindawi Publishing Corporation
Mathematical Problems in Engineering
Volume 2013, Article ID 956076, 11 pages
http://dx.doi.org/10.1155/2013/956076

Research Article

Mathematical Model and Analysis of Negative Skin Friction of Pile Group in Consolidating Soil

Gangqiang Kong,[1] Hanlong Liu,[1] Qing Yang,[2] Robert Y. Liang,[3] and Hang Zhou[1]

[1] *College of Civil and Transportation Engineering, Hohai University, Xikang Road No. 1, Nanjing, Jiangsu 210098, China*
[2] *State Key Laboratory of Coastal and Offshore Engineering, Dalian University of Technology, Dalian, Liaoning 116024, China*
[3] *Department of Civil Engineering, The University of Akron, Akron, OH 44325-3905, USA*

Correspondence should be addressed to Gangqiang Kong; gqkong1@163.com

Received 3 August 2013; Revised 10 October 2013; Accepted 11 October 2013

Academic Editor: Youqing Wang

In order to calculate negative skin friction (NSF) of pile group embedded in a consolidating soil, the dragload calculating formulas of single pile were established by considering Davis one-dimensional nonlinear consolidation soils settlement and hyperbolic load-transfer of pile-soil interface. Based on effective influence area theory, a simple semiempirical mathematical model of analysis for predicting the group effect of pile group under dragload was described. The accuracy and reliability of mathematical models built in this paper were verified by practical engineering comparative analysis. Case studies were studied, and the prediction values were found to be in good agreement with those of measured values. Then, the influences factors, such as, soil consolidation degree, the initial volume compressibility coefficient, and the stiffness of bearing soil, were analyzed and discussed. The results show that the mathematical models considering nonlinear soil consolidation and group effect can reflect the practical NSF of pile group effectively and accurately. The results of this paper can provide reference for practical pile group embedded in consolidating soil under NSF design and calculation.

1. Introduction

When vertical soil settlement is larger than that of pile, dragload (the additional compressive force) and downdrag (the excessive pile settlement) of pile caused by negative skin friction (NSF) occurred. It is one of common problems in the designing and construction of pile foundations in soft ground [1, 2]. In general, NSF on pile is caused by surcharge load or consolidating soil.

Previous studies results have shown that time effect were obviously presented on NSF on pile shaft caused by consolidating soil [3–9]. These studies were very helpful in understanding the NSF time effect behaviors of pile embedded in a consolidating soil, while few literatures focused on mathematical model analysis of NSF of pile embedded in a consolidating soil. NSF on pile shaft was increased with the increase of consolidation time and tended to be stabilized at last. Model tests and numerical simulation results have demonstrated that the dragload and downdrag on individual piles in a group was smaller than that on an isolated single pile because of group effect [10–13]. These studies were very helpful in understanding the behaviors of pile group under dragload. However, the literatures which focused on NSF group effect coefficient calculation method were scanty.

NSF theoretical research methods are mainly as follow: limit analysis method, elastic method, load-transfer (t-z curves) method, shear displacement method, mixed method, and variation method [14–18]. While a few of those methods consider the time effect of dragload and downdrag, less attention is given to group effect.

It was evident from the literature as cited above that most of the available studies were limited to empirical methods or numerical methods, while a few were on mathematical models or theoretical methods. Hence, there was a need to develop mathematical models to predict the NSF with considering time effect and the group effect of pile group. Such an analysis was presented in this study. The NSF on single pile calculating mathematical model was established by

considering Davis one-dimensional nonlinear consolidation soils settlement and hyperbolic load-transfer of pile-soil interface. One simple semiempirical mathematical model of analysis on predicting the group effect coefficient of pile group under NSF was described. In this group effect coefficient of mathematical model, the influence factors, such as, group arrange, pile space, soil type and its density, and pile-soil interface friction coefficient, were considered. The accuracy and reliability of mathematical models built in this paper were verified by practical engineering and model tests results comparative analysis. Then, the influences factors, such as, soil consolidation degree, the initial coefficient of volume compressibility, and the stiffness of end bearing soil, were analyzed and discussed.

2. Formula Built for Negative Skin Friction on Single Pile

2.1. Basic Assumptions. Soil was assumed as semi-infinite elastic body; foundation materials were assumed as homogeneous and isotropic materials. The radial deformation of pile and surrounding soils were ignored, and the consolidation processes of soils influenced by the driving of piles were not considered. Compressible homogeneous elastomers stress-strain relationship which obeys Hooke's law model was chosen for piles. Davis one-dimensional nonlinear consolidation theory model was chosen for the consolidation of soils. Hyperbolic load-transfer model and linear transfer model chosen for pile side-soils interface, and pile tip-soils interface mechanical transfer model, respectively.

Pile and its surrounding soil were chosen for research object in this paper, which was shown in Figure 1. The stress transferred from embankment to pile top was p, and to the surface ground was q, which means that pile-soil stress ratio equals p/q. The pile and its surrounding soil were divided into n unit in which node numbers i were from 1 to n. The elastic modulus and cross-sectional area of pile were E_p and A_p, respectively.

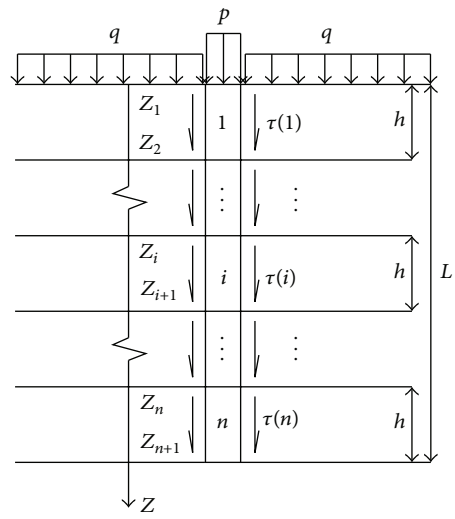

Figure 1: Mechanical model of a pile-soil system in pile-support embankment.

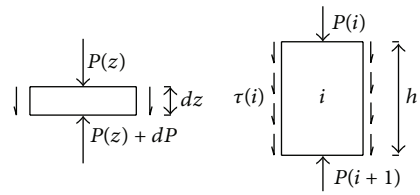

Figure 2: Bearing of pile segment and pile element.

2.2. Mechanical Model

(1) Control Equation of Pile-Soil System. The axial strain experienced by the pile can be related to the axial load by Hooke's law; the following equation can be obtained:

$$\frac{\partial w_p(z)}{\partial z} = -\frac{P(z)}{E_p A_p}, \tag{1}$$

where $P(z)$ is the axial force of pile at z depth, $w_p(z)$ is the settlement of pile at z depth, E_p is the elastic modulus of pile, and A_p is the cross-sectional area of pile.

Integrating (1) with limits (i) to $(i+4)$, the following can be obtained:

$$w_p(i) - w_p(i+1) = \frac{[P(i) + P(i+1)]\,h}{2E_p A_p}, \tag{2}$$

where $P(i)$ and $P(i+1)$ are the axial force of upper point of unit $i, i+1$, respectively; $w_p(i)$ and $w_p(i+1)$ are the settlement of upper point of unit i, $i+1$, respectively and h is the thickness of unit pile. The symbols schematic are shown in Figure 2.

Equation (2) can be rewritten into a matrix form:

$$\{P\} = [C]_p \left\{w_p\right\} + \{Q\}_p, \tag{3}$$

where $\{P\} = [P(1), P(2) \cdots P(n), P(n+1)]^T$ is the column vector of axial force of pile unit node, $\{wp\} = [wp(1), wp(2) \cdots wp(n), wp(n+1)]^T$ is the column vector of settlement of pile unit node, $\{Q\}_p = [Q, -Q \cdots (-1)^{n+2}Q]^T$ is the column vector of constant, and $[C]_p$ is the coefficient matrix.

(2) Pile Shaft-Soil Load-Transfer Model. The basic differential equations governing the deformation behavior of a compressible elastic pile under surcharge can be established by considering a small horizontal section as shown in Figure 1 as follows:

$$\frac{\partial P(z)}{\partial z} = -2\pi r_0 \tau(z), \tag{4}$$

where $\tau(z)$ is the side friction of pile at z depth and r_0 is the radius of pile.

Integrating (4), (5) can be obtained:

$$P(i+1) - P(i) = 2\pi r_0 \int_{z_i}^{z_{i+1}} \tau(z)\, dz = 2\pi r_0 h \tau(i), \quad (5)$$

where $\tau(i)$ is the side friction of unit i and z_i and z_{i+1} are the depth of unit i, $i+1$, respectively.

Equation (5) can be rewritten into a matrix form:

$$\{\tau\} = [C]_f \{w_p\} + \{Q\}_f, \quad (6)$$

where $\{\tau\} = [\tau(1), \tau(2) \cdots \tau(n)]^T$ is the column vector of side friction of pile unit node, $\{Q\}_f = [-Q/\pi r_0 h, Q/\pi r_0 h \cdots (-1)^n (Q/\pi r_0 h)]^T$ is the column vector of constant, and $[C]_f$ is the coefficient matrix.

Hyperbolic relationship between the friction of pile shaft and the relative displacement of pile and soil was chosen which is shown in

$$\tau(i) = \frac{\Delta(i)}{(1/k^i_{\text{ini}}) + (1/\tau^i_{\text{ult}})\Delta(i)}, \quad (7)$$

where $\Delta(i)$ is the average relative displacement of interface unit i, k^i_{ini} is the initial shear stiffness coefficient of interface unit i, which is determined by $k_{\text{ini}} = 2\pi Gl/\ln(r_m/r_0)$, G is the shear modulus of soil, l is the thickness of pile unit, r_m is the influence radius of pile, in which $r_m = 2\rho(1-\upsilon)L$, ρ is the ratio between shear modulus at the pile mid depth and shear modulus at pile tip, L is the pile length, υ is Poisson' ratio, τ^i_{ult} is the limit shear stress of interface unit i, which is determined by $\tau_{\text{ult}} = K_0 \sigma'_v \tan\delta = \beta \sigma'_v$, K_0 is the lateral pressure coefficient of soil, σ'_v is the vertical effective stress of surrounding soil, δ is the friction angle of pile-soil interface, and β is the coefficient of negative skin friction.

Equation (7) can be rewritten into a matrix form:

$$\{\tau\} = [K_s]\{\Delta\}, \quad (8)$$

where $\{\Delta\} = [\Delta(1), \Delta(2) \cdots \Delta(n)]^T$ is the average relative displacement of pile and soil, in which $\Delta(i) = [w_s(i) - w_p(i) + w_s(i+1) - w_p(i+1)]/2$, and $[K_s]$ is the coefficient matrix of pile side-soil load-transfer. Consider

$$[K_s] = \begin{bmatrix} k^1_s & & & \\ & k^2_s & & \\ & & \ddots & \\ & & & k^n_s \end{bmatrix}. \quad (9)$$

Substituting (8) into (6), the following equation can be obtained:

$$[K_s]\{\Delta\} - [C]_f \{w_p\} = \{Q\}_f. \quad (10)$$

(3) Pile-Bearing Soil Stratum Load-Transfer Model. Linear relationship between the tip resistance of pile and the relative displacement of pile and soil was chosen which is shown in

$$P_b = K_b S_b, \quad (11)$$

where P_b is the tip resistance of pile, S_b is the relative displacement of pile-soil at pile tip, where $S_b = w_p(n+1) - w_s(n+1)$, K_b is the coefficient function of pile tip load-transfer, where $K_b = \Psi E_s/2(1-\upsilon^2)r_0$, E_s is the compression modulus of soil, and coefficient $\Psi = 1 - (2\upsilon^2/1-\upsilon)$.

Combine (3), (10), and (11), then iterative solution. The axial force of pile $\{P\}$, side friction of pile $\{\tau\}$, and displacement of pile unit $\{w_p\}$ can be obtained.

(4) Consolidation Settlement of Surrounding Soil. Based on Davis one-dimensional nonlinear consolidation theory, excess pore water pressure of soil at z depth in t time, can be written as follows:

$$u(z,t) = \sigma\left[1 - \left(\frac{\sigma'_0}{\sigma}\right)^B\right] = \left(\sigma'_0 + q\right)\left[1 - \left(\frac{\sigma'_0}{\sigma'_0 + q}\right)^B\right], \quad (12)$$

where σ is the total stress, σ'_0 is the initial effective stress, and σ' and u are the effective stress and the pore water pressure in t time, respectively.

$$B = \sum_{N=0}^{N=\infty} \frac{2}{M} \sin\left(\frac{Mz}{H}\right) e^{-M^2 T_v}, \quad (13)$$

where $M = (2N+1)\pi/2$, N is the natural number, T_v is the time factor, where $T_v = C_v t/H^2$, C_v is the soil consolidation factor, and H is the thickness of drainage path.

The soil settlement with time and depth variation under uniform load can be expressed as follows:

$$S(z,t) = m_{v0}\sigma'_0 \ln\left(1 + \frac{q}{\sigma'_0}\right) \times H\left[1 - \frac{z}{H} - \sum_{N=0}^{N=\infty} \frac{2}{M^2} \cos\left(\frac{Mz}{H}\right) e^{-M^2 T_v}\right], \quad (14)$$

where m_{v0} is the initial volume compressibility, where $m_{v0} = C_c/\ln 10(1+e_0)\sigma'_0$, and C_c is the soil compression factor. ε is the vertical strain of soil, e is the void ratio of soil, and e_0 is the initial void ratio of soil.

3. Formula Built for Negative Skin Friction on Piles Group

3.1. Pile Group Effect Coefficient. For the purpose of explanation first assume that a given vertical pile group was arranged at a spacing S ($S < 6.0D$) in a rectangular arrangement as shown in Figure 3(a). Taking notice of a typical location of pile arrangement, it was possible to define the unit typical location of pile effective influence area as that shown on Figure 3(b). Then, consideration of the balance of forces in the vertical direction leads to (15) for the soil region whose horizontal section was single repeated in Figure 3(b) as follows:

$$\gamma' - \frac{d\sigma'_v}{dz} - \frac{\pi \tau_\alpha D}{A_i} = 0, \quad (15)$$

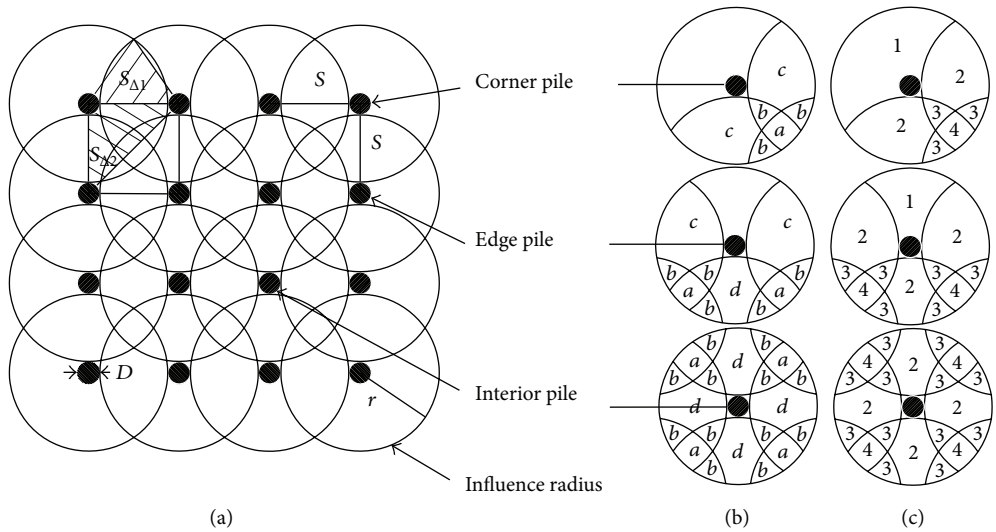

FIGURE 3: (a) Example of pile layout in rectangular arrangement, (b) effective influence areas of single typical location of piles and (c) overlap times of each influence area part.

where γ' is the submerged unit weight of soil, σ_v' is the vertical effective stress, z is the vertical coordinate, τ_α is the ultimate shaft friction, D is the pile diameter, and A_i is the influence area of soil. Note that the parameters A_i and τ_α are expressed as follows:

$$A_i = a\pi r^2 + b\pi D^2 + c(r + 0.5D)^2 + dC_1 + eC_2 + fC_3 + gC_4 \quad (i = 1, 2, 3), \tag{16}$$

where r is the influenced radius and D is the pile diameter, for corner pile $a = 3/4$, $b = -1/4$, $c = 1/4$, $d = -2$, $e = 1/2$, $f = 1/2$, and $g = -1/2$, edge pile $a = 1/2$, $b = -1/4$, $c = 1/2$, $d = -3$, $e = 3/4$, $f = 1$, and $g = -1$, interior pile $a = 0$, $b = -1/4$, $c = 1$, $d = -4$, $e = 1$, $f = 2$, and $g = -2$. Consider

$$C_1 = \frac{\pi r^2}{360}\arccos\left(\frac{r - D}{2r}\right),$$
$$C_2 = (r - D)^2 \tan\left(\arccos\frac{r - D}{2r}\right),$$
$$C_3 = r^2\arccos\frac{\sqrt{r^2 - 1/4(r + D/2)^2}}{r}, \tag{17}$$
$$C_4 = \sin\left[2\arccos\frac{\sqrt{r^2 - 1/4(r + D/2)^2}}{r}\right].$$

The influence areas of typical location of piles were shown in Table 1; the overlap times of each influence area part were shown in Figure 3(c).

The result of interior pile (P_I) was

$$A_{P_I} = -\frac{1}{4}\pi D^2 + \left(\frac{r + D}{2}\right)^2 - \frac{\pi r^2}{90}\arccos\left(\frac{r - D}{2r}\right) + (r - D)^2 \tan\left(\arccos\frac{r - D}{2r}\right) + 2r^2\arccos\frac{\sqrt{r^2 - 1/4(r + D/2)^2}}{r} - 2\sin\left[2\arccos\frac{\sqrt{r^2 - 1/4(r + D/2)^2}}{r}\right]. \tag{18}$$

The result of edge pile (P_E) was

$$A_{P_E} = \frac{1}{2}\pi r^2 - \frac{1}{4}\pi D^2 + \frac{1}{2}\left(\frac{r + D}{2}\right)^2 - \frac{\pi r^2}{120}\arccos\left(\frac{r - D}{2r}\right) + \frac{3}{4}(r - D)^2 \tan\left(\arccos\frac{r - D}{2r}\right) + r^2\arccos\frac{\sqrt{r^2 - 1/4(r + D/2)^2}}{r} - \sin\left[2\arccos\frac{\sqrt{r^2 - 1/4(r + D/2)^2}}{r}\right]. \tag{19}$$

Table 1: Influence areas of single piles.

Pile location	Influence area A_i
Interior pile (P_I)	$A_{P_I} = \pi r^2 - \frac{1}{4}\pi D^2 - \frac{1}{2}A_d \times 4 - \frac{2}{3}A_b \times 12 - \frac{3}{4}A_a \times 4$
Edge pile (P_E)	$A_{P_E} = \pi r^2 - \frac{1}{4}\pi D^2 - \frac{1}{2}A_c \times 2 - \frac{2}{3}A_b \times 6 - \frac{3}{4}A_a \times 2$
Corner pile (P_C)	$A_{P_C} = \pi r^2 - \frac{1}{4}\pi D^2 - \frac{1}{2}A_c \times 2 - \frac{2}{3}A_b \times 3 - \frac{3}{4}A_a$

The result of corner pile (P_c) was

$$\begin{aligned} A_{P_C} = {} & \frac{3}{4}\pi r^2 - \frac{1}{4}\pi D^2 + \frac{1}{4}\left(r + \frac{D}{2}\right)^2 \\ & - \frac{\pi r^2}{180}\arccos\left(\frac{r-D}{2r}\right) \\ & + \frac{1}{2}(r-D)^2 \tan\left(\arccos\frac{r-D}{2r}\right) \\ & + \frac{1}{2}r^2 \arccos\frac{\sqrt{r^2 - 1/4(r + D/2)^2}}{r} \\ & - \frac{1}{2}\sin\left[2\arccos\frac{\sqrt{r^2 - 1/4(r + D/2)^2}}{r}\right], \end{aligned} \tag{20}$$

$$\tau_\alpha = \sigma_h' \tan\phi_\alpha' = k\sigma_v' \tan\phi_\alpha', \tag{21}$$

where σ_h' is the horizontal effective stress, ϕ_α' is the angle of friction mobilized between pile and soil, and k is the ratio of the horizontal to the vertical effective stress.

Substitution of (21) into (15) yields

$$\frac{d\tau_\alpha}{dz} + \frac{\alpha\tau_\alpha \pi D}{A_i} = \alpha\gamma', \tag{22}$$

where $\alpha = k\tan\phi_\alpha'$. The boundary condition assumed here was

$$\tau_\alpha = \alpha p \text{ at } z = 0, \tag{23}$$

where p is the intensity of surface loading. Substitution of (23) into (22) yields

$$\tau_\alpha = \frac{\gamma' A}{\pi D}\left[1 - \exp\left(-\frac{\alpha\pi D z}{A_i}\right)\right] + \alpha p \exp\left(-\frac{\alpha\pi D z}{A_i}\right). \tag{24}$$

It should be noted here that putting the parameter uz/A to be zero in (24) restores the expression for the single pile; that is,

$$(\tau_\alpha)_{\text{single}} = \alpha\left(\gamma' z + p\right) = \alpha\sigma_v'. \tag{25}$$

Next, in order to express the degree of reducing dragload by installing piles in group, the group efficiency parameter η was introduced in the form

$$\eta = \frac{\int_0^{H_0} \tau_\alpha dz}{\int_0^{H_0} (\tau_\alpha)_{\text{single}} dz}, \tag{26}$$

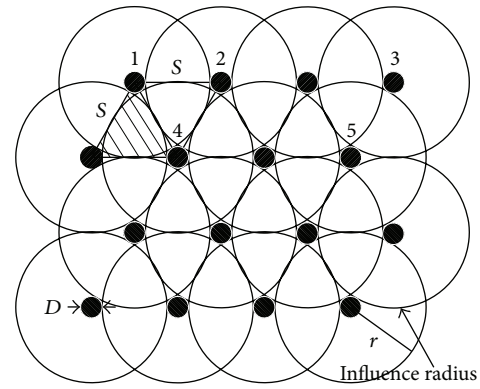

Figure 4: Example of pile layout in hexagonal arrangement.

where H_0 is the distance from the ground surface to the neutral plane of the given pile. Substitution of (24) and (25) into (26) allows the group efficiency parameter to be expressed as

$$\eta = \frac{p\left(1 - e^{-\chi}\right)/\chi + \gamma' H_0\left(\chi + e^{-\chi} - 1\right)/\chi^2}{p + \left(\gamma' H_0/2\right)}, \tag{27}$$

where $\chi = \alpha\pi D H_0/A_i$.

Use triangle of hatched sections ($S_{\Delta 1}$ and $S_{\Delta 2}$) which were shown in Figure 3(a) to calculate the effective influence area. The simplified style of A_i was obtained. Its precision results satisfied the demands of practical engineering. Consider

$$A_i = \pi r^2 - \frac{1}{4\pi D^2} - a_i S^2, \quad i = 1 \sim 3, \tag{28}$$

where a_i equal to 0.77, 1.77, and 2.70 and i equal to 1, 2, and 3, respectively. S is the spacing of pile.

Pile groups were arranged in a hexagonal arrangement which were shown in Figure 4. From the same reasoning as stated above it can be concluded that (27) applies to the pile group of hexagonal pattern as well, provided that the parameter A_i was modified as follows.

And for the need of practical engineering, the area of the hatched section was calculated by the triangle instead of curve side triangle. Then,

$$A_i = \pi r^2 - \frac{1}{4\pi D^2} - a_i S_\Delta, \quad i = 1 \sim 5, \tag{29}$$

where a_i is equal to 7/3, 3, 5/3, 4, and 11/3 from $i = 1$ to 5, respectively. $S_\Delta = 0.433 \times S^2$.

Table 2: Physical and mechanical parameters of soils on site.

Name	Depth/m	Density/(kN·m^{-3})	Compression modulus/MPa	Cohesion/kPa	Internal friction angle (°)
Clay	1.86	18.4	4.61	24.5	8.7
Muddy clay	2.54	18.3	7.55	8.4	6.3
Clay	4.86	20.0	9.39	37.3	16.7
Silt with silty sand or clay	5.70	19.0	10.01	15.6	21.0
Silty clay	8.70	18.2	6.08	14.7	15.3
Silty sand	20.0	19.5	28.25	4.0	20.0

Before closing this subsection it may be appropriate to supplement that (27) reduced to (30a), when the surface loading term (p-term) dominates, whereas (27) reduced to (30b), when the body-force term ($\gamma' H_0$-term) dominates. Consider

$$\eta = \frac{\left(1 - e^{-\chi}\right)}{\chi}, \tag{30a}$$

$$\eta = \frac{2\left(\chi + e^{-\chi} - 1\right)}{\chi^2}, \tag{30b}$$

for $S > 6.0D$, $\eta = 1$.

3.2. Pile Group Calculation. Based on the above analyze, the dragload and downdrag of pile group can be obtained as follows:

$$F_G = \eta \times n \times F_S, \tag{31a}$$

$$S_G = \eta \times n \times S_S, \tag{31b}$$

where F_G is the dragload of pile group, F_S is the dragload of single pile; S_G is the downdrag of piles group, S_S is the downdrag of single pile, n is the number of piles.

4. Theoretical Model Verification

4.1. Single Pile Calculation Method. In order to verify the accuracy and reliability of the suggested mathematical model, one of field tests investigating on negative skin friction of pile on soft ground was comparatively analyzed [24]. Drilled shaft with 43 m long and 1.0 m diameter, was loaded by 5.05 m embankment fill height that was constructed in the site. Physical and mechanical parameters of soils on site are shown in Table 2. The bulk density of filled soils equals 21.5 kN/m^3, the stiffness modulus of pile (E_p) equals 25 GPa, the coefficient of soil consolidation (C_v) equals 5.4×10^{-6} m^2/s, the initial volume compressibility factor (m_{v0}) equals 1.5×10^{-4} m^2/kN, base coefficient of pile tip (K_b) equals 23.1 MPa/m, the coefficient of negative skin friction (β) equals 0.3, and Poisson's ratio (υ) of soil equals 0.3.

The relative displacement of pile-soil contact surface has nonlinear relationship with friction of pile shaft; hence,

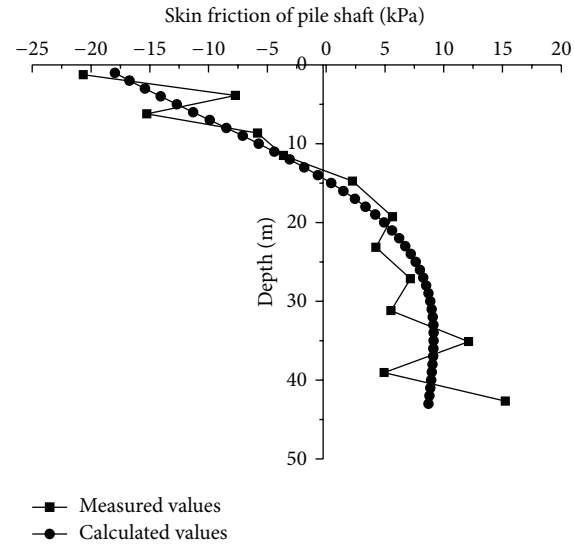

Figure 5: Comparative curves of negative skin friction of pile shaft between calculated and measured results.

secant shear stiffness coefficient (k_s) was used in load-transfer function shown in

$$k_s^i = \frac{\tau(i)}{\Delta(i)} = \frac{k_{\text{ini}}^i \tau_{\text{ult}}^i}{\tau_{\text{ult}}^i + k_{\text{ini}}^i \Delta(i)}, \tag{32}$$

where k_{ini} is the initial value of shear stiffness coefficient k_s, $\Delta(i)$ is the mean value of relative displacement, and absolute value was chosen in iterative calculation process.

Take the end of embankment filling (4.5 months after embankment filling) for an example; the friction of pile shaft and axial force of pile which is obtained by field test and calculated method are shown in Figures 5 and 6, respectively. The stress ratio of pile-soil on the end of embankment filling equals about 4.5. The pile top load and surcharge load of measured equal 487.9 kPa and 108.6 kPa, respectively. Figure 5 shows that the friction of pile shaft calculated by proposed method in this paper is similar to that obtained on field test. Above neutral plane, the friction of pile shaft nearly increased on linear; below neutral plane, the friction of pile shaft increased on nonlinear. The measured value near the bottom of the pile is improved greatly; it may be because of the enhancement effect on the pile tip. Figure 6 shows that the axial force of pile calculated by mathematical model is similar to that obtained by field test. The maximum value of axial force of pile is occurred on about 14 m deep. In other

Table 3: The details of the pile arrangements, parameters, and principal items regarding each pile test.

Source of data	Pile code*	Pile arrangement	Pile length H/m	S/D	H_0/D
Kong et al. [19]	1 2 3	3 × 3	0.7	4.0	17.1
Little [20]	1 3	3 × 3	20.4	4.0	27.6
	1 3	3 × 3	20.8	4.0	30.7
Combarieu [21]	1 2 3	3 × 4	20.0	3.54	40.0
Shibata et al. [22]	1 2 3	3 × 3	0.7	2.50	9.0
Okabe [23]	4 5 6 7	38**	40.0	2.11	49.3 43.6 43.6 43.6

*The pile code for the relative position of the piles within the group shown in Figure 7.
**Hexagonal arrangement.

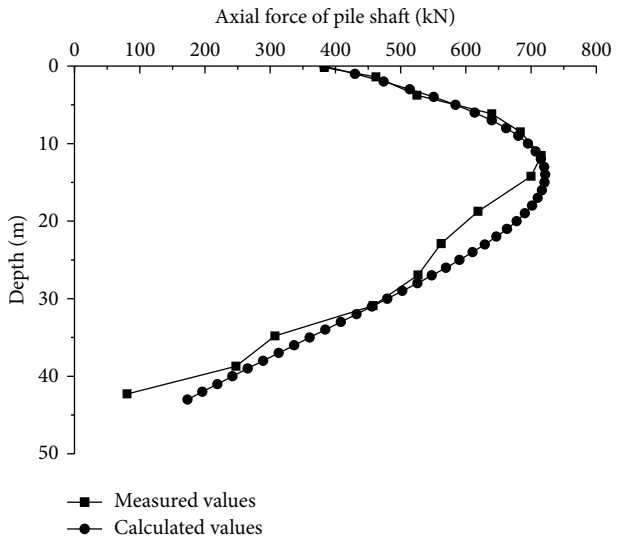

Figure 6: Comparative curves of axial force of pile between calculated and measured results.

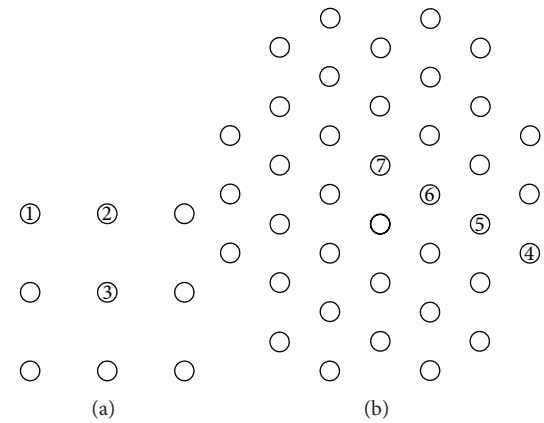

Figure 7: Arrangement of pile group and the code of typical piles, (a) rectangular arrangement (b) hexagonal arrangement.

words, the neutral plane of calculated by mathematical model equals 14.4 m; the neutral plane of measured value by field test is between 11.5 to 14.7 m.

4.2. Piles Group Calculation Method. In order to verify the accuracy and reliability of pile group calculated method, series field tests and model tests results on dragload comparative analysis were taken out. The details of the pile arrangements were shown in Figure 7, and the principal items regarding each pile test were showed in Table 3.

(1) Example Case Studied by Kong et al. One 3 × 3 piles group with pile spacing equals 4.0D (D equal to 0.041 m) was presented by Kong et al. [19] (for the position of piles, refer to Figure 7(a)). The model piles were driven to 0.7 m clay, approximately 0.2 m above the silt layer. For the surrounding clay layer, the soil modulus E_s equals 2.01 MPa, the unit weight of soil (γ) equals 17.4 kN/m^3, and the effective cohesion (c_{cu}) and effective friction angle (φ_{cu}) equal 7.0 kPa and 19.1°, respectively. For the stratum silt layer, the soil modulus E_s equals 2. 31 MPa, the unit weight of soil (γ) equals 13.9 kN/m^3, the effective cohesion (c_{cu}) and effective friction angle (φ_{cu}) equals 16.2 kPa and 33.9°, respectively. The surface load equals 5.1 kPa. The pile-soil interface friction coefficient (μ) was found to be 0.59 from the direct shear test. The results of measured and predicted values are shown in Figure 8.

(2) Example Case Studied by Little. Two 3 × 3 piles groups (one friction pile type and one end-bearing pile type) with pile spacing equals 4.0D (D equals 0.406 m) field test on

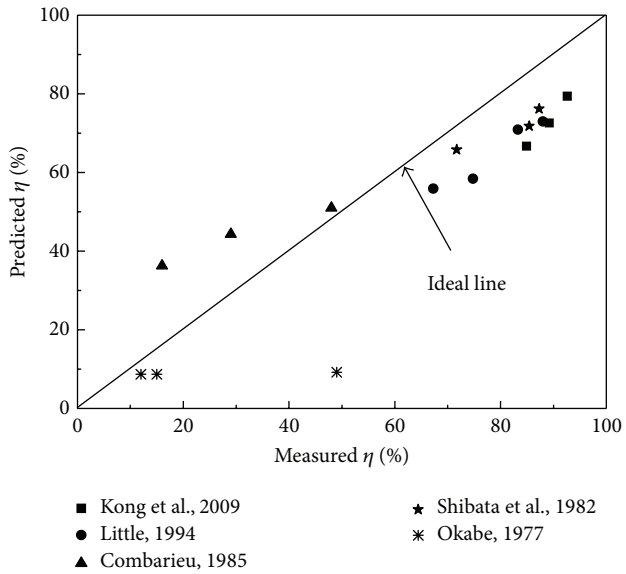

FIGURE 8: Comparisons of the group efficiency parameter η obtained by measured and predicted values.

dragloads were presented by Little [20]. (for the position of piles, refer to Figure 7(a)). The friction piles were driven to 20.4 m, approximately 1 m above the gravel layer. The end-bearing piles were driven onto the gravel layer; the piles length were 20.8 m. The soil modulus E_s of 3.5 MPa was back-calculated for the clay layer from the measured ground settlement (180 mm). The interface friction coefficient μ of 0.35 was used. Assume that the submerged unit weight of soil (γ') equals 9 kN/m^3, the value of α equals 0.3, the effective cohesion (c') equals 3.0 kN/m^2, and effective friction angle (φ') equals 25°. An embankment loading of 40 kPa was applied on the top of the clay after driving the piles. The results of measured and predicted values are shown in Figure 8.

(3) Example Case Studied by Combarieu and Jeong. One 3×4 piles group with $3.54D$ pile spacing field test on dragloads was presented by Combarieu [21] and Jeong [25]. The model pile length (L) equals 20 m and pile diameter (D) equals 0.5 m. The soil properties were as follows: the submerged unit weight of soil (γ') equals 18 kN/m^3, the value of α equals 0.3, the effective cohesion (c') equals 30.0 kN/m^2, and the surface load (p) equals 200 kPa. Assuming a K value of 0.6-0.7 for normally consolidated clay and a β value of 0.3 as given by Combarieu, a rough estimate for interface friction coefficient (μ) equales 0.4 and 0.5 was obtained. The stiffness modulus (E_s) of clay was taken to be 5 and 10 MPa, respectively. The results of measured and predicted values are shown in Figure 8.

(4) Example Case Studied by Shibata et al. Model tests for a single pile and piles in group were carried out by Shibata et al. [22]. The model steel pipe piles with an outer diameter (D) of 0.06 m, a length (L) of 0.7 m, and wall thickness (d) of 1.2 mm were carried out. The pile group consisted of 3×3 piles with a spacing (S) of $2.5D$ (for pile positions, refer to Figure 7(a)). Assume that the modulus of the steel pipe pile (E_p) equals 15.7×10^6 kPa. The piles were assumed to be end-bearing. The clay model was formed from kaolin slurry under self-weight consolidation, which had the following index properties: w_L equals 52%, w_p equals 39%, clay fraction equals 39%, and specific gravity equals 2.61. The effective unit weight of the clay slurry (γ') equals 5.3 kN/m^3. A surface loading of 20 kPa was applied on the top of the clay surface to produce soil settlement after completion of the self-weight consolidation. The soil modulus (E_s) of 150 kPa was assumed from the consideration of measured soil settlement (65 mm). The measured results showed that the dragload of single pile reached to 410 N after consolidation; the corner pile, edge pile, and central pile of 3×3 pile group reached to 358 N, 350 N, and 294 N, respectively. The group effects results of measured and predicted values are shown in Figure 8.

(5) Example Case Studied by Okabe. Field test on dragload in a pile group, resulting from a combination of draining and surcharge loading was reported by Okabe [23]. The pile group consisted of 38 piles with $2.11D$ pile spacing, the diameter of pile (D) was 0.71 m, and embedded lengths (L) were 40 m (for the arrangement of pile group see Figure 7(b)). There were 14 external piles that can be free to move; it takes most of the NSF; the other 24 internal end-bearing piles are connected to a rigid pile cap. After installation of the piles, the embankment as a surcharge was placed on a very soft clay layer with SPT N-values of 0–10 and unconfined compressive strength of 0–110 kN/m^2 from 0 to 40 m depth. Below the soft clay was a medium sandy gravel layer with N-values of about 50. Ground settlement was reported both by the fill and dewatering from the underlying aquifer for urban water supply. The properties of the soft clay were assumed. The submerged unit weight of soil (γ') equals 18 kN/m^3, the value of α equals 0.3, the soft clay Young's modulus (E_s) equals 5 MPa, the effective cohesion (c') equals 5.0 kN/m^2, and effective friction angle (φ') equals 25°. The soil settlement reached 10 cm at ground surface after 300 days at a 5.6 m surcharge placement, and the surface load (p) equals 250 kPa. The results of measured and predicted values are shown in Figure 8.

Computations of group efficiency parameter η value were made by using (27) and (28) for the pile group of rectangular arrangement and (27) and (29) for the pile group of hexagonal arrangement. Comparative pile group efficiency parameters obtained by using the present method and field test results reported by various investigators are shown in Figure 8. It is evident from Figure 8 that there is a good agreement between the measured and predicted values of the group efficiency parameter.

5. Parametric Analysis

Based on the pile and soil parameters shown in Section 4.1, series influence factors, such as, soil consolidation degree, initial volume compressibility coefficient of surrounding soil, soil stiffness of pile base, and pile-soil stress ratio, were analyzed and discussed.

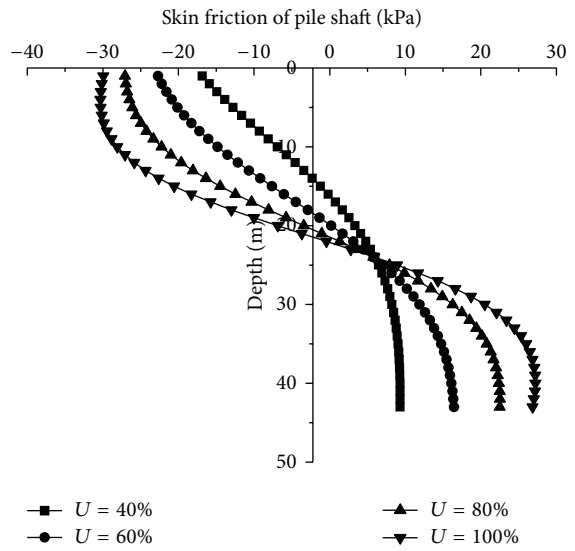

Figure 9: Curves of skin friction versus pile depth influenced by soil consolidation degree.

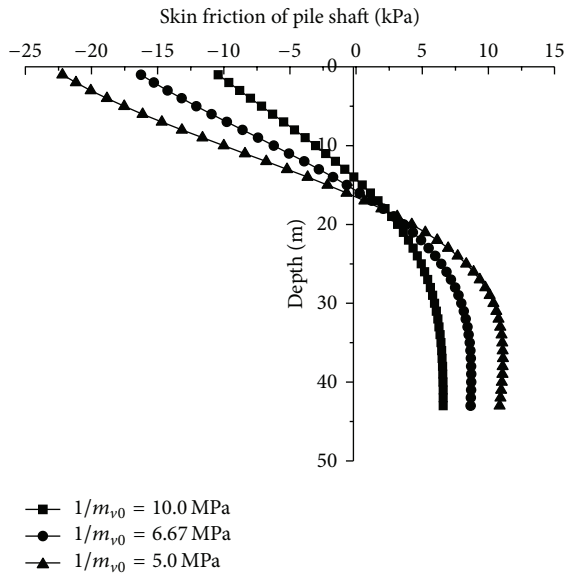

Figure 10: Curves of skin friction versus pile depth influenced by initial volume compressibility coefficient.

5.1. Influence of Soil Consolidation Degree. The relationships of skin friction versus pile depth influenced by soil consolidation degree were shown in Figure 9. It shows that the neutral plane position is a little higher in the beginning of consolidation time than that in the end of consolidation time; the neutral plane position increased with consolidation time increasing. In other words, the areas of negative skin friction gradually expanded with consolidation time. In this analysis condition, the neutral plane position increased from 16.2 m to 22.1 m, with increase ratio nearly equals 36.4%. It also shows that the neutral plane position becomes a stable value after a long period of consolidation time; neutral plane position has an obvious time effect.

5.2. Influence of Initial Volume Compressibility Coefficient of Surrounding Soil. For the same soil consolidation degree, the skin friction and neutral plane position influenced by different initial volume compressibility coefficient (m_{v0}) of surrounding soil are shown in Figure 10. It shows that the negative skin friction increased with initial volume compressibility coefficient increasing neutral plane position increased with initial volume compressibility coefficient increasing. In this analysis condition, the neutral plane position increased from 14.2 m to 16.6 m, with increase ratio of nearly 16.9%. In other words, the negative skin friction is obviously influenced by the initial volume compressibility coefficient.

5.3. Influence of Bearing Soil Stiffness. The negative skin friction and neutral plane position influenced by different soil stiffness of pile base (K_b) are shown in Figure 11. It shows that the neutral plane position increased with soil stiffness of pile base increasing. In this analysis condition, the neutral plane position increased from 13.8 m to 18.2 m, with increase ratio nearly equals 31.9%. In other words, soil stiffness of pile base is one of key influence factors to neutral plane position.

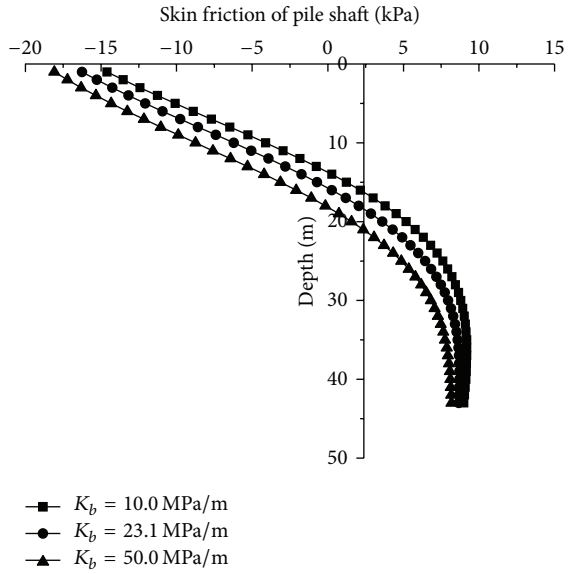

Figure 11: Curves of skin friction versus pile depth influenced by soil stiffness of pile base.

5.4. Influence of Pile-Soil Stress Ratio. In the same soil consolidation degree, the maximum axial force of pile, maximum dragload, tip resistance, and neutral plane position influenced by different pile-soil stress ratio were shown in Table 4. It shows that maximum axial force of pile increased with pile-soil stress ratio increasing, the maximum dragload decreased with pile-soil stress ratio increasing, and the tip resistance increased with pile-soil stress ratio increasing. It also shows that neutral plane position increased with pile-soil stress ratio increasing. When pile-soil stress ratio increased, more load-transfers to pile top, which leads to the settlement of pile. This new pile settlement leads to the relative displacement

Table 4: Dragload and neutral plane position influenced by different pile-soil stress ratio calculated by mathematical model.

Pile-soil stress ratios	Maximum axial force of pile/kN	Maximum dragload/kN	Tip resistance/kN	Neutral plane position/m
3.0	717.3	461.3	184.7	16.9
4.5	755.6	402.4	201.9	15.7
6.0	857.9	346.3	221.0	14.5

of pile-soil. Hence, the neutral plane position increased and maximum dragload decreased.

6. Conclusions and Discussions

In this paper, one NSF of single pile calculating formula and one group effect coefficient calculating formula were described. Based on case studies and influence factors analysis, the following conclusions can be drawn.

(1) In the simple mathematical models on negative skin friction of single pile calculation method and group efficiency parameter calculation method built in this paper, physical meaning is clear, calculated process is simple and operable, and the parameters in the formula are easy to obtain, especially for the simplified effective influence area which is according to engineering demand. In the calculation method, nonlinear soil consolidation settlement can be considered in negative skin friction of single pile. Pile group arrangement, embedment length to diameter ratio of piles, pile spacing, soil properties such as angle of internal friction, density, and pile-soil interface friction coefficient can be considered in group efficiency parameter of pile group. Case studies show that the calculated results and measured data from previous observations are in excellent agreement, which indicates that the presented approach is feasible for applications in engineering practice.

(2) Negative skin friction and neutral plane position exists a significant time effect its values increased with consolidation time increasing, and eventually they tends toward stable values. Neutral plane position is obviously influenced by soil consolidation degree and soil stiffness of pile base. In this paper's analysis condition, the neutral plane position increased nearly 36.4% when 2.5 times soil consolidation degree increased; the neutral plane position increased nearly 31.9% when 5 times soil stiffness of pile base increased.

(3) Increasing pile-soil stress ratio leads to a reduction in pile-soil relative movement, which decreases the negative skin friction on pile shaft.

Disclosure

This work is an original one conducted at Hohai University. The work described has not been submitted elsewhere for publication, in whole or in part.

Conflict of Interests

The authors declare that there is no conflict of interests regarding the publication of this paper.

Authors' Contribution

All the authors have contributed to and approved this paper.

Acknowledgments

The authors wish to thank the National Science Foundation of China (no. 51278170, U1134207), the Program for Changjiang Scholars and Innovative Research Team in University (no. IRT1125) and the 111 Project (no. B13024) for financial support.

References

[1] B. H. Fellenius, "Results from long-term measurement in piles of drag load and downdrag," *Canadian Geotechnical Journal*, vol. 43, no. 4, pp. 409–430, 2006.

[2] H. G. Poulos, "A practical design approach for piles with negative friction," *Proceedings of the Institution of Civil Engineers*, vol. 161, no. 1, pp. 19–27, 2008.

[3] T. M. Toma, *A model study of negative skin friction on a fixed base pile in soft clay [Ph.D. thesis]*, Heriot-Watt University, Edinburgh, Scotland, 1989.

[4] A. M. Hanna and A. Sharif, "Drag force on single piles in clay subjected to surcharge loading," *International Journal of Geomechanics*, vol. 6, no. 2, pp. 89–96, 2006.

[5] D. M. K. N. Kunitaki, B. S. L. P. De Lima, A. G. Evsukoff, and B. P. Jacob, "Probabilistic and fuzzy arithmetic approaches for the treatment of uncertainties in the installation of torpedo piles," *Mathematical Problems in Engineering*, vol. 2008, Article ID 512343, 26 pages, 2008.

[6] S. Y. Lam, C. W. W. Ng, C. F. Leung, and S. H. Chan, "Centrifuge and numerical modeling of axial load effects on piles in consolidating ground," *Canadian Geotechnical Journal*, vol. 46, no. 1, pp. 10–24, 2009.

[7] L.-M. Wang, J.-J. Sun, X.-F. Huang, S.-H. Xu, Y.-C. Shi, and R.-D. Qiu, "A field testing study on negative skin friction along piles induced by seismic subsidence of loess," *Soil Dynamics and Earthquake Engineering*, vol. 31, no. 1, pp. 45–58, 2011.

[8] W. Yao, Y. Liu, and J. Chen, "Characteristics of negative skin friction for superlong piles under surcharge loading," *International Journal of Geomechanics*, vol. 12, no. 2, pp. 90–97, 2012.

[9] S. Lam, C. W. W. Ng, and H. Poulos, "Shielding piles from downdrag in consolidating ground," *Journal of Geotechnical and Geoenvironmental Engineering*, vol. 139, no. 6, pp. 956–968, 2013.

[10] Y. M. EI-Mossallamy, A. M. Hefny, M. A. Demerdash, and M. S. Morsy, "Numerical analysis of negative skin friction on piles in soft clay," *HBRC Journal*, vol. 9, no. 1, pp. 68–76, 2013.

[11] C. J. Lee, M. D. Bolton, and A. Al-Tabbaa, "Numerical modelling of group effects on the distribution of dragloads in pile foundations," *Geotechnique*, vol. 52, no. 5, pp. 325–335, 2002.

[12] C. J. Lee and C. W. W. Ng, "Development of downdrag on piles and pile groups in consolidating soil," *Journal of Geotechnical and Geoenvironmental Engineering*, vol. 130, no. 9, pp. 905–914, 2004.

[13] C. W. W. Ng, H. G. Poulos, V. S. H. Chan, S. S. Y. Lam, and G. C. Y. Chan, "Effects of tip location and shielding on piles in consolidating ground," *Journal of Geotechnical and Geoenvironmental Engineering*, vol. 134, no. 9, pp. 1245–1260, 2008.

[14] J. E. Garlanger and T. W. Lambe, "Proceedings of a symposium on downdrag of piles," Tech. Rep. 73-56, MIT, Cambridge, Mass, USA, 1973.

[15] C. I. Tah and K. S. Wong, "Analysis of downdrag on pile groups," *Geotechnique*, vol. 45, no. 2, pp. 191–207, 1995.

[16] W. Y. Shen and C. I. Teh, "A variational solution for downdrag force analysis of pile groups," *International Journal of Geomechanics*, vol. 2, no. 1, pp. 75–91, 2002.

[17] R. P. Chen, W. H. Zhou, and Y. M. Chen, "Influences of soil consolidation and pile load on the development of negative skin friction of a pile," *Computers and Geotechnics*, vol. 36, no. 8, pp. 1265–1271, 2009.

[18] W. Cao, Y. Chen, and W. Wolfe, "A new load transfer hyperbolic model for pile-soil interface and negative skin friction on single piles embedded in soft soils," *International Journal of Geomechanics*, 2013.

[19] G.-Q. Kong, Q. Yang, P.-Y. Zheng, and M.-T. Luan, "Evaluation of group effect of pile group under dragload embedded in clay," *Journal of Central South University of Technology*, vol. 16, no. 3, pp. 503–512, 2009.

[20] J. A. Little, "Downdrag on piles: review and recent experimentation," in *Proceedings of the Conference on Vertical and Horizontal Deformations of Foundations and Embankments*, pp. 1805–1826, Geotechnical Special Publication, New York, NY, USA, June 1994.

[21] O. Combarieu, "Frottement négatif sur les pieux, Rapport de recherche LCPC," Tech. Rep. 136, Laboratoire Central des Ponts et Chaussées, Paris, France, 1985.

[22] T. Shibata, H. Sekiguchi, and H. Yukitomo, "Model test and analysis of negative skin friction acting on piles," *Soils and Foundations*, vol. 22, no. 2, pp. 29–39, 1982.

[23] T. Okabe, "Large negative friction and friction-free pile methods," in *Proceedings of the 9th International Conference on Soil Mechanics and Foundation Engineering*, pp. 679–682, Tokyo, Japan, 1977.

[24] W.-T. Lu, W.-M. Leng, and Y.-H. Wang, "In-situ tests on negative friction resistance of abutment piles in soft soil," *Chinese Journal of Geotechnical Engineering*, vol. 27, no. 6, pp. 642–645, 2005.

[25] S. Jeong, *Nonlinear three dimensional analysis of downdrag on pile groups [Ph.D. thesis]*, Texas A & M University, College Station, Tex, USA, 1992.